SciEn

Proceedings of 8th International Conference on Mechanical, Industrial and Energy Engineering 2024
02-04 January, 2025, Khulna, BANGLADESH

SciEn Conference Series: Engineering Vol. 3, 2025, pp 191-196 https://doi.org/10.38032/scse.2025.3.50

Improving Thermal Management of Li-ion Batteries in Electric Vehicles: A CFD Study of a Hybrid System with Nanofluid and Peltier Module

Md. Ahnaf Adit[1], *Md Mahamudul Hasan Pranto*[1, *], *Samiul hasan*[1], *Yousuf Abir Bari*[1], *Sadia Tasneem*[2]

[1] Department of Mechanical Engineering, Rajshahi University of Engineering & Technology, Rajshahi-6204, Bangladesh
[2] Department of Mechatronics Engineering, Rajshahi University of Engineering & Technology, Rajshahi-6204, Bangladesh

ABSTRACT

Efficient thermal management is crucial for optimizing the performance, safety, and longevity of lithium-ion batteries in electric vehicles (EVs). This study introduces a novel hybrid Battery Thermal Management System (BTMS) that integrates nanofluid and Peltier module to enhance heat dissipation and maintain optimal temperature ranges. The system operates in a closed-loop configuration, where the nanofluid circulates to absorb heat from the battery and is subsequently cooled by the Peltier module before being recirculated. Using Computational Fluid Dynamics (CFD), alongside the Newman Tiedemann Gu and Kim (NTGK) model, the thermal behavior was simulated in ANSYS Fluent. The thermal profile of the 32140 Series 15 Ah Li-ion cell illustrates the highest internal maximum temperature and cell surface temperature at discharge rate 10C, followed by 7C and 5C, respectively. The CuO/DI water nanofluid was prepared at 0.1 w/v% concentration with a surfactant-to-nanoparticle weighted ratio of 1:2.5. Furthermore, the nanofluid sample exhibits a maximum enhancement in thermal conductivity of 9.928% relative to deionized water, which justifies its application in thermal applications like BTMS. The proposed BTMS effectively reduced the maximum temperature rise of the cell 32140. Compared to the temperature rise observed without BTMS, the reductions achieved were as follows: 1.6% at a 5C discharge rate, 10.8% at a 7C discharge rate, and 19.5% at a 10C discharge rate. The findings emphasize the system's potential to extend battery life by minimizing degradation rates. This research highlights the potential of integrating nanofluids and Peltier modules in advanced BTMS designs, offering a promising approach to enhance the operational stability and safety of Li-ion batteries in EV applications.

Keywords: Lithium-ion, BTMS, CFD analysis, Nanofluid.

1. Introduction

The growing market for electric vehicles (EVs) has considerably raised the necessity for effective thermal management system in lithium-ion (Li-ion) batteries to guarantee safety, performance, and durability. To achieve optimal performance, it is advisable to sustain the working temperature between 15 and 35 ºC [1]. To prevent rapid battery capacity deterioration and thermal runaway, the temperature must be sustained between 60 °C and 80 °C [2]. To maintain the efficacy and reliability of the battery, a battery thermal management system (BTMS) is necessary. This method guarantees secure functionality and superior charging-discharging efficiency [3]. Computational Fluid Dynamics (CFD) is widely employed techniques for simulating BTMS. CFD simulations provide insights into temperature distribution within battery packs, crucial for optimizing thermal management [4]. In contrast to basic thermal models, the Newman, Tiedemann, Gu and Kim (NTGK) model incorporate the nonlinear heat generation rates resulting from fluctuations in the state of charge (SOC), current load, and temperature [5]. Standard cooling methods for BTMS encompass liquid cooling, air cooling, phase change materials (PCMs), and hybrid systems. Liquid cooling demonstrates significant efficiency, as indicated by a study showing that a module-level liquid cooling system markedly reduced maximum temperatures [6]. Nanofluids are increasingly used in battery thermal management systems (BTMS) due to their superior heat transfer characteristics and ability to enhance the cooling performance. They enable more efficient heat dissipation, help maintain uniform temperature distribution, and can be integrated with other cooling techniques like phase change materials and heat pipes which leads to enhanced battery performance, extended lifespan, and improved safety in various applications, including electric vehicles [7], [8]. Torregrosa et al. [9] shown that the incorporation of CuO nanoparticles with phase change materials enhanced heat dissipation. This combination yielded a notable 28% enhancement in heat transfer efficiency. Ranjan et al. [10] examined the utilization of PCM combined with Al_2O_3 nanoparticles at various weight percentages. Their research shown that n-PCM at a 4% weight fraction, along with air cooling, reduced the battery temperature by 40%. The incorporation of a Peltier module in BTMS can significantly reduce the peak cell temperature, hence improving battery longevity and efficiency [11]. Pakrouh et al. [12] introduced a novel liquid-based battery thermal management system that integrates phase change material and thermoelectric cooling. The thermoelectric module effectively controls the temperature of the battery pack, achieving a reduction ranging from 11.3°C to 17.75°C. Williams et al. [13] found that the incorporation of Peltier cooling in battery systems improves thermal uniformity, maintaining temperature variations among cells at a mere 1.2°C. Hybrid thermal management systems integrate different cooling techniques, optimizing

*Corresponding Author Email Address: pmahamud1983@gmail.com

temperature regulation of Li-ion batteries in electric vehicles more efficiently than singular solutions, resulting in enhanced performance and sustainability [14]. Despite extensive research on BTMS for various cylindrical cells, a significant gap exists in the design and analysis of BTMS specifically tailored for 32140 cells. To the best of the authors' knowledge, no prior work has proposed or evaluated a BTMS design for this cell type. Furthermore, the cooling mechanism of battery cell developed in this study is unique, presenting a novel approach to managing thermal performance in 32140 cells.

This work aims to develop a hybrid battery thermal management system (BTMS) utilizing a CAD model optimized for high energy density cylindrical lithium-ion cells. This system will employ advanced nanofluids and a Peltier module for thermal management. The principal objective is to regulate the cell temperature within an appropriate range to mitigate degradation and avert thermal runaway, hence extending the cell's lifespan.

2. Methodology

2.1. Material Preparation

Nanofluid was prepared using the two-step method which is the most widely employed method by the researchers [15]. Here, CuO nanoparticles (ranging in size from 40 to 60 nm) were dispersed in the base fluid, DI water, with the addition of surfactant SDS. CuO nanoparticles have been chosen due to their cost-effectiveness and market availability; additionally, SDS is utilized as a surfactant to enhance nanoparticle dispersion, hinder agglomeration, and improve wettability, resulting in superior thermal conductivity, heat transfer, and corrosion resistance in diverse systems [16], [17]. A distinct sample of nanofluid with surfactant-to-nanoparticle weighted ratios of 1:2.5 was prepared at 0.1 w/v% concentration. The increased surfactant concentration notably decreases the thermal conductivity of the nanofluid; hence, the surfactant-to-nanoparticle ratio was kept at 1:2.5 to use a lesser quantity of surfactant compared to nanoparticles [18]. Following the mixing of base fluid, nanoparticles, and surfactant in a beaker, magnetic stirring was done for 1 hour (at 50^{o}C and 2400 rpm), and ultrasonication was done for 10 hours (using an ultrasonication bath) for further proper dispersion of nanoparticle in the base fluid. Magnetic stirring assisted the premixing of the nanoparticle, base fluid and surfactant, while ultrasonication was employed for a prolonged duration compared to magnetic stirring to ensure adequate dispersion of the nanofluid through ultrasonic vibration [19], [20].

2.2. BTMS Design

The Battery Thermal Management System (BTMS) was developed on SOLIDWORKS 2023. Fig.1 represents the full setup of the BTMS. The cell has an aluminum shell around it for better conduction of heat from the top and bottom portion of the cell. Aluminum was selected for its higher thermal conductivity[21]. The BTMS consists of a cylindrical ring surrounding the shell, designed to facilitate heat transfer from the shell via fluid flow. This ring was considered to be made of a thermally insulated material. A copper chamber is positioned with its base in contact with the cold side of a Peltier module, ensuring effective heat absorption. Copper was chosen for its better thermal conduction[22]. The remaining surfaces of the copper chamber, as well as the entire system except for the surface in contact with the Peltier module, are insulated to prevent heat exchange with the environment. This ensures that the fluid does not absorb heat from the surroundings if the environmental temperature is higher than the fluid temperature. The pump, cylindrical ring, and copper chamber are connected via pipes in a closed-loop system to maintain continuous fluid flow, enabling efficient heat transfer. Table 1 highlights the dimensions of essential segments of the BTMS module. The full setup dimensions were determined based on the dimensions of the battery cell, the Peltier module and the minimum ring structure required. Fig. 1 presents a schematic depiction of the Battery Thermal Management System (BTMS), highlighting multiple perspectives.

Table 1 Dimension of the different parts of the BTMS.

Part	Shape/Model	Dimension (mm)	No used
Aluminum Chamber	Cylindrical	Inner dia. = 32 Outer dia. = 36 Height = 140	2
Ring	Cylindrical	Inner dia. = 36 Outer dia. = 56 Height = 30	1
Battery	32140 Series 15 Ah Lithium ion	Diameter = 32 Length = 140	1
Pump		Diameter = 50 Length = 70	1
Peltier	TEC-12703	Length = 40 Width = 40	1
Cubic Copper Chamber		Length = 40 Width = 40 Height = 40	1
Pipe		Diameter =12	2
Solenoid Valve		Inner Diameter =14 Outer Diameter =12	1

In this BTMS, the fluid inside the ring structure and connecting pipes will be pumped into the chamber containing the Peltier cooler. During this process, the solenoid valve will remain closed to allow the chamber to fill completely. Once the chamber is filled, the fluid will be precooled by the Peltier cooler before the continuous cooling cycle begins during cell discharge. After precooling, the solenoid valve will open, allowing the cooled liquid to flow out of the chamber and into the pipes and ring structure. This process will leave the Peltier chamber with a very low level of fluid, as the continuous cooling cycle with a constant flow rate starts. During this cycle, the cooled liquid will circulate to reduce the temperature of the cell as it discharges and generates heat.

2.3. CFD Analysis

This study built a CFD model for a battery temperature management system utilizing Ansys 2023. The preliminary stage entailed determining the heat generation rate for a 32140 Series 15 Ah Li-ion cell using MSMD battery model in Ansys Fluent. Modeling lithium-ion batteries is complex due to their multi-domain, multi-physics nature and varying length scales. The MSMD (Multiscale Multidimensional) approach manages these challenges by solving physics in their respective domains. MSMD approach depends on some chemical sub-models and NTGK (Newman, Tiedemann, Gu, and Kim) is one of them [23]. This model is capable of calculating transfer current density, phase potentials, joule heating, electrochemical heating and entropic heating [24].

The cell material specifications were derived from the cell datasheet [25]. The cell, possessing a capacity of 15 Ah, accommodates discharge rates of up to 10C. The operational voltage range was established with a minimum stop voltage of 2V and a maximum of 3.2V [26].

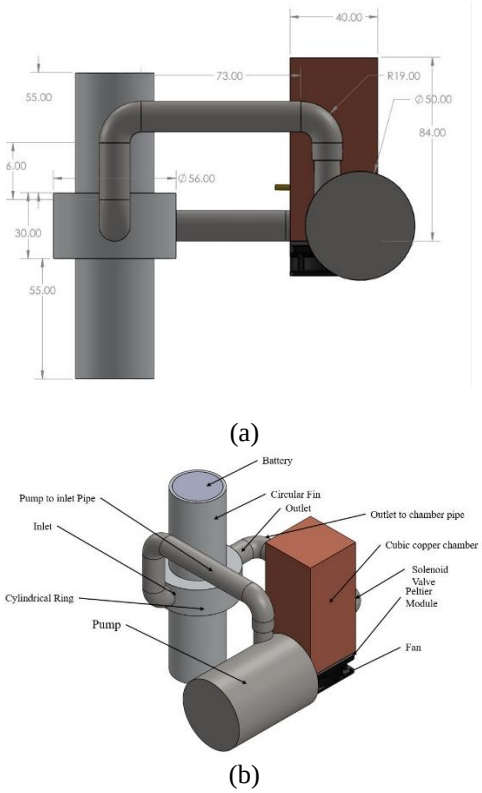

Fig.1 (a) Dimensions in millimeter of BTMS model and (b) BTMS model different sections.

After determining the heat generation rate cooling simulations of the proposed BTMS were performed at different C-ratings, with a constant mass flow rate of 0.1145 kg/s for the working fluid. An aluminum cylindrical shell was used for thermal management to enhance conduction. The fluid domain walls were treated as insulated during the simulation. BTMS simulations initiated at an initial temperature of 300K, with the nanofluid inlet pre-cooled to 293K. Free convection due to air flow was neglected in the boundary conditions of simulation. Both NTGK modeling and BTMS simulations employed the viscous SST k-omega turbulence model as the CFD solver, offering a comprehensive understanding of fluid dynamics and heat transmission inside the system.

3. Results and Discussion

3.1. Nanofluid properties

For characterization of prepared nanofluid samples, various thermophysical properties are measured including thermal conductivity, density, viscosity and specific heat. Among these, thermal conductivity is the most important property for any thermal application. Transient hot wire method (THW) is employed here to measure the thermal conductivity of prepared nanofluid by varying temperatures. It is evident from the Table 2 that, thermal conductivity value increases as the temperature rises, maximum thermal conductivity of prepared sample was found 0.7207 W/mK at 70 ºC. The produced CuO/DI nanofluid exhibited a maximum thermal conductivity enhancement of 9.928% compared to DI water. The density and viscosity were measured, as these influence the necessary pumping power for recirculation. The nanofluid exhibits a marginally greater density than water, yet possesses a lower viscosity. Considering that water has a density of 997 kg/m³ and a viscosity of approximately 1 mPa·s at 25ºC [27], this indicates that the nanofluid enhances thermal management efficiency while maintaining similar pumping power demands. Stability of nanofluid is inspected by visual observation method. Fig. 2 illustrates the condition of nanofluid after fixed time interval, which indicates that nanofluid is in well stable condition after 90 days.

Table 2 Different thermophysical properties of prepared CuO/DI nanofluid sample.

Properties	Temperature (ºC)	Value
Thermal Conductivity ($W \cdot m^{-1} \cdot K^{-1}$)	30	0.6543
	40	0.6786
	50	0.6896
	60	0.7061
	70	0.7207
Density ($Kg \cdot m^{-3}$)	31	1034.4
Viscosity (mPas)	25	0.897
Specific Heat ($J \cdot kg^{-1} \cdot K^{-1}$)	25	4.178

Fig.2 Visual observation of prepared nanofluid sample.

3.2. Validation of the numerical model

Two curves were evaluated to assess mesh dependency in NTGK modeling and the cooling simulation in ANSYS Fluent, as depicted in Fig. 3. In NTGK modeling, the curve illustrates the heat generation rate as a function of the element count. Similarly in the cooling simulation, the curve indicates the peak surface temperature as a function of the number of elements at 10C.

The results indicated that varying the number of elements caused less than a 1% change in both heat generation rate and surface temperature. An element size of 1 mm was selected for both simulations as it significantly reduced computational cost while enhancing the resolution and smoothing the temperature contour. Using a 1 mm element size resulted in 634,245 elements for the cooling simulation and 240,172 elements for NTGK modeling. The mesh quality was acceptable for both NTGK modeling and BTMS simulation. Both mesh had a skewness less than 0.8 and orthogonality greater than 0.2. The NTGK model was validated by simulating the heat generation rate of a 26650 cell, as presented in the paper [28]. In that study, the authors measured the cell's heat generation rate using a heat flux sensor and reported an average value of 307,000 W/m³ at a 9.6 C-rate. When the NTGK model was applied to

simulate the heat generation rate for the same cell, the average value obtained was 311,343 W/m³, resulting in an error of approximately 1.414%.

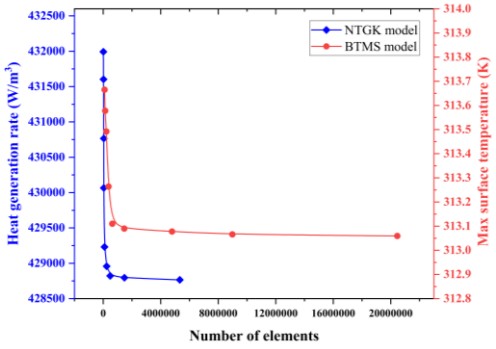

Fig.3 Mesh dependency analysis.

3.3. NTGK modeling of cell

The cell's behavior during discharge at different rates was examined by the NTGK model. Fig.4 illustrates the volumetric heat generation rate within the cell with respect to time. At higher C-rating the current through the cell is also higher. Due to internal resistance cell generates heat inside the cell. The cell internal temperature increases due to lower radial conductivity of the cellular substance. The NTGK modeling revealed average heat generation rates of 204,065 W/m³ at 5C, 382,531 W/m³ at 7C, and 763,999 W/m³ at 10C. The derived values were thereafter employed as energy sources in the source term options of the cell zone conditions. The average heat generation rate was used in the cooling simulation instead of using NTGK model to generate heat to reduce the computational time.

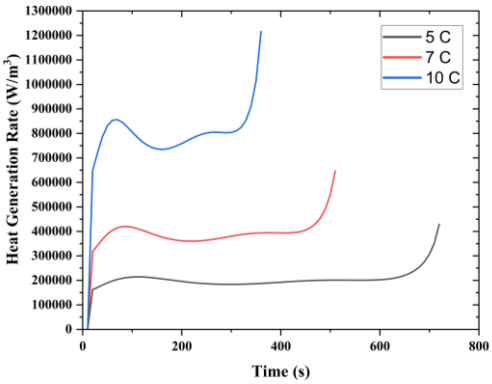

Fig.4 Heat generation rate of the cell with respect to time for different discharge rates.

3.3. Thermal profile of cell

Fig.5 shows the maximum internal temperature of the cell with BTMS over time at various discharge rates. Fig.6 shows the rise in temperature with time at different C-rating with and without BTMS. Fig.7, 8, and 9 illustrate the temperature contours of a cell both with and without the BTMS at various discharge rates. Table 3 presents the temperature rise of the cell surface with and without BTMS at various discharge rates. Analyzing Table 3 it is evident that temperature rise reduced significantly to 1.6%, 10.8% and 19.5% of the original temperature rise without BTMS. The NTGK modeling was initialized at 296K rather than 300K due to the fact that the data sheet of the cell recorded data starting from 296K.

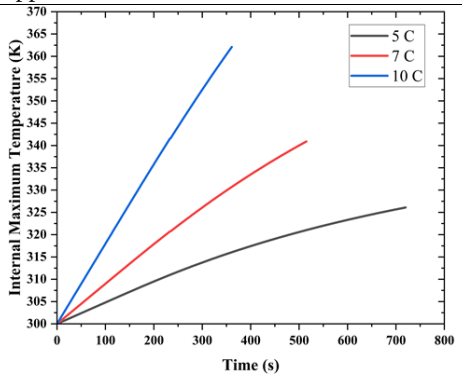

Fig.5 Cell internal temperature with BTMS as function of time.

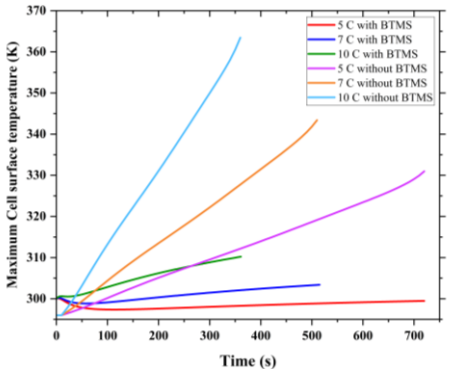

Fig.6 Cell surface temperature as function of time with and without BTMS.

Table 3 Surface temperature rise of the cell with and without BTMS at various discharge rates.

C-rating	Initial cell temperature (K)		Maximum surface tempera-ture rise without BTMS (K)	Maximum surface tempera-ture rise with BTMS (K
	With BTMS	Without BTMS		
5C	300	296	34.98	0.558
7C	300	296	47.4	5.143
10C	300	296	67.47	13.17

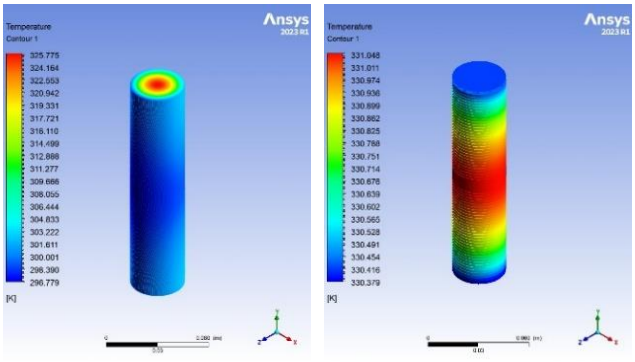

(a) (b)

Fig.7 Temperature contour of (a) cell with BTMS and (b) cell without BTMS at 5C.

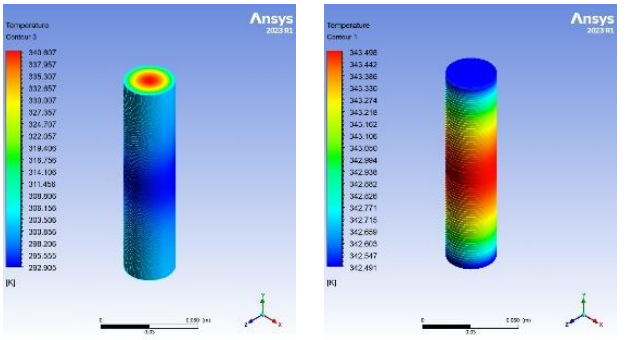

(a) (b)

Fig.8 Temperature contour of (a) cell with BTMS and (b) cell without BTMS at 7C.

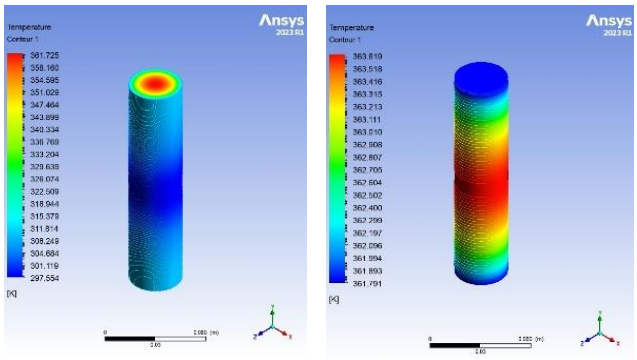

(a) (b)

Fig.9 Temperature contour of (a) cell with BTMS and (b) cell without BTMS at 10C.

4. Conclusion

The development and evaluation of a hybrid Battery Thermal Management System (BTMS) integrating nanofluid and Peltier module demonstrated significant advancements in thermal management for lithium-ion batteries in electric vehicles. Here, by using NTGK module, the highest average heat generation was found 763,999 W/m^3 at 10C, followed by 382,531 W/m^3 at 7C, 204,065 W/m^3 at 5C discharge rate respectively. Moreover, both internal cell surface temperature and internal maximum temperature was found highest at discharge rate 10C, which followed by discharge rate sequentially at 7C and 5C. The reason behind the maximum temperature at discharge rate 10C is the raised current amplifies heat production due to increased internal resistance losses, resulting in higher cell temperatures compared to 7C and 5C rates. The prepared CuO/DI nanofluid exhibited a maximum thermal conductivity improvement of 9.928% compared to DI water, with stability observed for up to 90 days. Finally, the system effectively controlled the temperature rise during battery discharge, achieving a reduction in temperature rise. Temperature rise reduced to 1.6%, 10.8% and 19.5% of original temperature rise without BTMS at discharge rates of 5C, 7C, and 10C, respectively. This reduction in temperature helped maintain battery temperatures within a safer operational range, mitigating the risks associated with thermal runaway and improving overall safety.

Future work should aim to extend this approach to battery pack configurations to assess scalability and real-world applicability. This simulated model must be optimized before fabrication so that it can save energy and enhance cooling for different battery cell model. Further exploration of different nanofluids, enhanced materials, and system designs could lead to even greater thermal management efficiency, contributing to the advancement of sustainable electric vehicle technologies.

References

[1] Suresh Kumar, OM Prakash Shukla, and Jaydeep Shah, "Thermal management lithium-ion battery for electric vehicles with using cold plate," *World Journal of Advanced Engineering Technology and Sciences*, vol. 12, no. 1, pp. 087–094, May 2024

[2] Divya D Shetty, Mahamad Sulthan, Mohammad Zuber, Irfan Anjum Badruddin, and Chandrakant R Kini, "Computational Design and Analysis of a Novel Battery Thermal Management System of a Single 26650 Li-Ion Battery Cell for Electric Vehicle Application," *Journal of Advanced Research in Fluid Mechanics and Thermal Sciences*, vol. 93, no. 2, pp. 61–75, Apr. 2022

[3] D. Zou *et al.*, "Preparation of a novel composite phase change material (PCM) and its locally enhanced heat transfer for power battery module," *Energy Convers Manag*, vol. 180, pp. 1196–1202, Jan. 2019

[4] M. Shendre and V. Kumar, "Electro-Thermal Simulation Methodology for Battery Thermal Management System (BTMS) Performance Evaluation of Li-Ion Battery Electric Vehicles," Sep. 2023.

[5] M. Jeong, H. Lee, J. Yoon, and W.-S. Yoon, "O3-type NaNi1/3Fe1/3Mn1/3O2 layered cathode for Na-ion batteries: Structural evolution and redox mechanism upon Na (de) intercalation," *J Power Sources*, vol. 439, p. 227064, Nov. 2019

[6] W. Wei, Z. Luo, S. Qiao, J. Zhai, and Z. Lei, "Analysis and design of module-level liquid cooling system for rectangular Li-ion batteries," *Int J Heat Mass Transf*, vol. 225, p. 125435, Jun. 2024

[7] B. Venkateswarlu, S. C. Kim, S. W. Joo, and S. Chavan, "Numerical Investigation of Nanofluid as a Coolant in a Prismatic Battery for Thermal Management Systems," *J Therm Sci Eng Appl*, vol. 16, no. 3, Mar. 2024

[8] S. G. Sankeeth, S. Kathiresan, J. Harish, D. Srihari, and R. Harish, "Comparison of Heat Transfer Characteristics of Nanofluids for Electric Vehicle Battery Thermal Management," 2023, pp. 57–68

[9] A. J. Torregrosa, A. Broatch, P. Olmeda, and L. Agizza, "Analysis of the improvement of a lithium-ion battery module cooling system employing nanofluid and nano encapsulated phase change materials by means of a lumped electro-thermal model," *J Energy Storage*, vol. 70, p. 107995, Oct. 2023

[10] R. Ranjan, R. Kumar, and T. Srinivas, "Thermal performance of nano-enhanced phase change material and air-based lithium-ion battery thermal management system: An experimental investigation," J Energy Storage, vol. 82, p. 110567, Mar. 2024

[11] M. Vachhani, K. R. Sagar, D. N. Jha, Vipul. M. Patel, and H. B. Mehta, "Cooling hybrid/electric vehicle battery module: exploring the thermal potential of single evaporator Loop heat Pipe," *Energy Sources, Part A: Recovery, Utilization, and Environmental Effects*, vol. 46, no. 1, pp. 689–705, Dec. 2024.

[12] R. Pakrouh, M. J. Hosseini, A. A. Ranjbar, and M. Rahimi, "A novel liquid-based battery thermal management system coupling with phase change material and thermoelectric cooling," *J Energy Storage*, vol. 64, p. 107098, Aug. 2023

[13] N. P. Williams, D. Trimble, and S. M. O'Shaughnessy, "An experimental investigation of liquid immersion cooling of a four cell lithium-ion battery module," *J Energy Storage*, vol. 86, p. 111289, May 2024

[14] A. Rahmani, M. Dibaj, and M. Akrami, "Recent Advancements in Battery Thermal Management Systems for Enhanced Performance of Li-Ion Batteries: A Comprehensive Review," *Batteries*, vol. 10, no. 8, p. 265, Jul. 2024

[15] W. T. Urmi, A. S. Shafiqah, M. M. Rahman, K. Kadirgama, and M. A. Maleque, "Preparation Methods and Challenges of Hybrid Nanofluids: A Review," *Journal of Advanced Research in Fluid Mechanics and Thermal Sciences*, vol. 78, no. 2, pp. 56–66, Dec. 2020

[16] J. Du, Y. Wang, W. Yang, J. Wang, Z. Cao, and B. Sundén, "Effect of nanoparticle concentration and surfactants on nanofluid pool boiling," *Int J Heat Mass Transf*, vol. 221, Dec. 2023, doi: 10.1016/j.ijheatmasstransfer.2023.125080.

[17] P. Pandian *et al.*, "Effect of sodium dodecyl sulfate surfactant on the surface properties of electroless NiP-TiO2-ZrO2 composite coatings on magnesium AZ91D substrate," *Arabian Journal of Chemistry*, vol. 16, May 2023.

[18] A. Rehman *et al.*, "Effect of surfactants on the stability and thermophysical properties of Al2O3+TiO2 hybrid nanofluids," *J Mol Liq*, vol. 391, p. 123350, Dec. 2023.

[19] B. Mehta, D. Subhedar, H. Panchal, and K. K. Sadasivuni, "Stability and thermophysical properties enhancement of Al2O3-water nanofluid using cationic CTAB surfactant," *International Journal of Thermofluids*, vol. 20, Jun. 2023.

[20] M. Sandhya, D. Ramasamy, K. Sudhakar, K. Kadirgama, and W. S. W. Harun, "Ultrasonication an intensifying tool for preparation of stable nanofluids and study the time influence on distinct properties of graphene nanofluids – A systematic overview," *Ultrason Sonochem*, vol. 73, Feb. 2021

[21] S. K. Pradhan *et al.*, "Graphene-incorporated aluminum with enhanced thermal and mechanical properties for solar heat collectors," AIP Adv, vol. 10, Jun. 2020

[22] C. Subramaniam *et al.*, "Carbon nanotube-copper exhibiting metal-like thermal conductivity and silicon-like thermal expansion for efficient cooling of electronics," *Nanoscale*, vol. 6, Jan. 2014.

[23] K. H. Kwon, C. B. Shin, T. H. Kang, and C.-S. Kim, "A two-dimensional modeling of a lithium-polymer battery," *J Power Sources*, vol. 163, no. 1, pp. 151–157, Dec. 2006

[24] U. Seong Kim, J. Yi, C. B. Shin, T. Han, and S. Park, "Modeling the Dependence of the Discharge Behavior of a Lithium-Ion Battery on the Environmental Temperature," *J Electrochem Soc*, vol. 158, no. 5, p. A611, 2011

[25] H. Yu *et al.*, "Thermal parameters of cylindrical power batteries: Quasi-steady state heat guarding measurement and thermal management strategies," *Appl Therm Eng*, vol. 231, Aug. 2023

[26] "Applications • Electric 2 & 3 Wheelers • Light Commercial Vehicles (eLCV) • Electric Utility Vehicles • Hybrid-Electric Marine • UPS and Telecom Backup • Residential Energy Storage • Material Handling and AGVs • Industrial Equipment 32140 Lithium Ion Energy Cell," 2024. [Online]. Available: www.lithiumwerks.com/contact

[27] B. Zhang, X. Zhao, J. Zhang, J. Wang, and H. Jin, "An investigation of the density of nano-confined subcritical/supercritical water," *Energy*, vol. 284, Sep. 2023

[28] S. J. Drake *et al.*, "Heat generation rate measurement in a Li-ion cell at large C-rates through temperature and heat flux measurements," *J Power Sources*, vol. 285, pp. 266–273, Jul. 2015

NOMENCLATURE

- c : Specific heat, $J \cdot Kg^{-1} \cdot K^{-1}$
- C : Cell discharge rating
- k : Thermal Conductivity, $W \cdot m^{-1} \cdot K^{-1}$
- m : Mass flow rate, $Kg \cdot s^{-1}$
- q' : Heat Generation Rate, $W \cdot m^{-3}$
- T : Temperature, K
- t : Time, s
- μ : Viscosity, mPas
- ρ : Density, $Kg \cdot m^{-3}$
- σ : Electrical conductivity, $S \cdot m^{-1}$
- Q : Cell capacity, Ah